Journal of Inorganic Biochemistry 117 (2012) 77–84

Contents lists available at SciVerse ScienceDirect

Journal of Inorganic Biochemistry

journal homepage: www.elsevier.com/locate/jinorgbio

A novel organobismuth compound, 1-[(2-di-*p*-tolylbismuthanophenyl)diazenyl] pyrrolidine, induces apoptosis in the human acute promyelocytic leukemia cell line NB4 via reactive oxygen species

Kengo Onishi [a], Mizuho Douke [a], Taisuke Nakamura [a], Youta Ochiai [a], Naoki Kakusawa [b], Shuji Yasuike [b,*], Jyoji Kurita [b], Chika Yamamoto [b], Masatoshi Kawahata [c], Kentaro Yamaguchi [c,*], Tatsuo Yagura [a,**]

[a] Department of Bioscience, Faculty of Science and Technology, Kwansei Gakuin University, 2-1, Gakuen, Sanda, 669-1337, Japan
[b] Faculty of Pharmaceutical Science, Hokuriku University, Kanagawa-machi, Kanazawa 920-1181, Japan
[c] Faculty of Pharmaceutical Sciences at Kagawa Campus, Tokushima Bunri University, Shido, Sanuki 769-2193, Japan

ARTICLE INFO

Article history:
Received 23 May 2012
Received in revised form 4 September 2012
Accepted 4 September 2012
Available online 12 September 2012

Keywords:
Organobismuth
Triazene
Human cancer cell
Apoptosis
ROS

ABSTRACT

A novel organobismuth compound, 1-[(2-di-*p*-tolylbismuthanophenyl)diazenyl]pyrrolidine (**4**), which has 1-(phenyldiazenyl)pyrrolidine (**1**) substituent in a benzene ring of tri(*p*-tolyl)bismuthane (**2**), was synthesized and tested for biological activity toward human tumor cell lines. **4** had a potent anti-proliferative effect on human cancer cell lines, although both **1** and **2** exhibited only weak activity. The sensitivity of leukemic cell lines to **4** was relatively high; IC_{50} values for the human leukemia cell line NB4 and cervical cancer cell line HeLa were 0.88 μM and 5.36 μM, respectively. Treatment of NB4 cells with **4** induced apoptosis, loss of mitochondrial membrane potential ($\Delta\Psi_{mt}$) and the generation of cellular reactive oxygen species (ROS). **1** and **2** did not induce apoptosis and had only a marginal effect on $\Delta\Psi_{mt}$ and the generation of ROS. N-acetyl cysteine (NAC) reduced the generation of ROS and conferred protection against **4**-induced apoptosis, indicating a role for oxidative stress. **4** did not inhibit the polymerization of tubulin *in vitro*. 1-[2-(di-p-tolylstibanophenyl)diazenyl]pyrrolidine (**3**), which has the same chemical structure as **4** but contains antimony in place of bismuth, did not show any cytotoxic activity. The results suggest that the conjugated structure of the diazenylpyrrolidine moiety and bismuth center are key to the bioactivity of **4**.

1. Introduction

Alkylating agents can be used in cancer chemotherapy though they are carcinogenic. Triazenes possessing cytotoxic alkylating effects have been known to show anticancer activity [1–8]. Clinical studies show that triazenes exhibit anti-neoplastic activity in patients with acute leukemia [9–11]. Through metabolic activation, dacarbazin (DTIC), a triazene, generates a cytotoxic monomethyl triazene species that alkylates DNA [3,4,12–14]. Temozolomide, a tetranitrogen heterocycle that spontaneously decomposes into a monomethyl metabolite without metabolic activation, showed significant clinical activity against high-grade glioma [15]. On the other hand, a series of synthesized chemical compounds with a triazene moiety exhibits antimalarial activity [16]. These studies suggest the triazene moiety to be crucial to interaction with many cellular targets.

Over the last several years, our laboratory has engaged in the study of chemically synthesized bismuth-based organometallic compounds with anticancer activity and has shown that their antiproliferative activity varies dependent on chemical structure [17,18]. These studies should lead to the development of new organobismuth compounds with stronger and more selective biological activity for future applications in medicine.

In the present study, as a part of a search for new organometalloid compounds with excellent anticancer activities, we synthesized a triarylbismuth(III) compound with a diazenyl pyrrolidine (a triazene structure) substitute at the *ortho* position, based on tri(*p*-tolyl) bismuthane which showed only low biological activity [see review, 19], and explored its cytotoxic activity against human acute promyelocytic leukemia (APL) cell line, NB4. The purpose was to determine whether the substitute could enhance the biological activity or provide insight into how organobismuth compounds exert their antiproliferative activity toward cancer cells. We found that the cytotoxic activity of tri(*p*-tolyl)bismuthane **2** was markedly enhanced by the introduction of a diazenyl pyrrolidine moiety. The present results might open the way to the design of a new type of therapeutic agent based on organobismuth compounds.

* Corresponding authors.
** Corresponding author. Tel./fax: +81 79 565 8473.
E-mail addresses: s-yasuike@hokuriku-u.ac.jp (S. Yasuike), yamaguchi@kph.bunri-u.ac.jp (K. Yamaguchi), tyagura@kwansei.ac.jp (T. Yagura).

0162-0134/$ – see front matter © 2012 Elsevier Inc. All rights reserved.
http://dx.doi.org/10.1016/j.jinorgbio.2012.09.009

2. Experimental

2.1. Synthesis: general procedures and materials

Melting points were taken on a Yanagimoto micro melting point hot-stage apparatus (MP-S3) and are not corrected. ^{1}H NMR (tetramethylsilane: δ: 0.00 as an internal standard) and ^{13}C NMR ($CDCl_3$: δ: 77.00 as an internal standard) spectra were recorded on a JEOL JNM-ECA400 (400 MHz and 100 MHz) in $CDCl_3$ unless otherwise stated. Mass spectra (MS) were obtained on a JEOL JMS-DX300 (70 eV, 300 μA). All chromatographic separations were accomplished with Silica Gel 60 N (Kanto Chemical Co., Inc.). Thin-layer chromatography (TLC) was performed with Macherey–Nagel Pre-coated TLC plates Sil G25 UV_{254}. 1-(Phenyldiazenyl)pyrrolidine (**1**) [20] and tri(*p*-tolyl)bismuthane (**2**) [21] were prepared according to reported procedures.

2.1.1. Synthesis of 1-[2-(di-p-tolylstibanophenyl)diazenyl]pyrrolidine (**3**)

To a solution of 1-[(2-iodophenyl)diazenyl]pyrrolidine (903 mg, 3 mmol) in tetrahydrofuran (30 ml) was *n*-BuLi (3.1 ml, 5.1 mmmol, 1.65 mol/l in hexane) at −78 °C under an argon atmosphere added, and the solution was stirred for 20 min at the same temperature. A solution of p-Tol_2SbBr [prepared from tri(*p*-tolyl)stibane (1.58 g, 4 mmol) and tribromoantimony (722 mg, 2 mmol)] in ether (20 ml) was then added dropwise with stirring over a 15 min period at −78 °C. After an additional 2 h of stirring at the same temperature, the mixture was allowed to warm slowly to room temperature, then stirred for another 18 h. Ether (50 ml) and water (50 ml) were added to the reaction mixture with stirring at 0 °C. The resulting organic layer was separated and the aqueous layer was extracted with ether (50 ml×2). The combined organic layer was washed with brine, dried over anhydrous $MgSO_4$, and evaporated *in vacuo*. The residue was subjected to column chromatography on silica gel with a mixture of hexane and dichloromethane (5:3) to give **3** as colorless prisms with hexane and ether (5:2). **3**: 582 mg, 40% yield, mp 127–130 °C. ^{1}H NMR ($CDCl_3$) δ 1.90 (m, 4H, 2×CH_2), 2.31 (s, 6H, 2×Tol), 3.38 (br, 2H, CH_2), 3.79 (br, 2H, CH_2), 6.69 (t, 1H, J=7.3Hz, Ar–H), 7.07 (d, 1H, J=7.3 Hz, Ar–H), 7.08 (d, 4H, J=7.8 Hz, Ar–H), 7.30 (t, 1H, J=7.3 Hz, Ar–H), 7.31 (d, 4H, J=7.8 Hz, Ar–H), and 7.51 (d, 1H, J=7.3 Hz, Ar–H). ^{13}C NMR ($CDCl_3$) δ: 21.4 (q), 23.5 (br), 46.5 (br), 51.7 (br), 116.2 (d), 125.7 (d), 129.3 (d), 129.4 (d), 135.6 (d), 135.7 (s), 136.1 (s), 136.5 (d), 137.5 (s), and 154.1 (s). Electron ionization-mass spectrometry (EI-MS) *m/z*: 477 (M^+), anal. (%) calcd. for $C_{24}H_{26}N_3Sb$: C, 60.27; H, 5.48; N, 8.79; found: C, 60.35; H, 5.43; N, 8.74.

2.1.2. Synthesis of 1-[2-(di-p-tolylbismuthanophenyl)diazenyl] pyrrolidine (**4**)

To a solution of 1-[(2-iodophenyl)diazenyl]pyrrolidine (903 mg, 3 mmol) in tetrahydrofuran (30 ml) was *n*-BuLi (3.2 ml, 5.3 mmmol, 1.65 mol/l in hexane) at −78 °C under an argon atmosphere added, and the solution was stirred for 20 min at the same temperature. A suspension of p-Tol_2BiCl [prepared from tri(*p*-tolyl) bismuthane (964 mg, 2 mmol) and trichlorobismuthane (315 mg, 1 mmol)] in ether (15 ml) was then added dropwise with stirring over a 10-min period at −78 °C. After an additional 2 h of stirring at the same temperature, the mixture was allowed to warm slowly to room temperature, then stirred for another 16 h. Ether (50 ml) and water (50 ml) were added to the reaction mixture with stirring at 0 °C. The resulting organic layer was separated and the aqueous layer was extracted with ether (30 ml×2). The combined organic layer was washed with brine, dried over anhydrous $MgSO_4$, and evaporated *in vacuo*. The resulting solids were recrystallized from a mixture of hexane and ether (5:1) to give **4** as colorless prisms (808 mg, 48% yield), mp 136–139 °C. ^{1}H NMR ($CDCl_3$) δ: 1.93 (m, 4H, 2×CH_2), 2.30 (s, 6H, 2×Tol), 3.47 (br, 2H, CH_2), 3.80 (br, 2H, CH_2), 7.05 (t, 1H, J=6.9 Hz, Ar–H), 7.14 (d, 4H, J=7.5 Hz, Ar–H), 7.32 (t, 1H, J=6.9 Hz, Ar–H), 7.60 (d, 4H, J=7.5 Hz, Ar–H), 7.62 (d, 1H, J=6.9 Hz, Ar–H), and 7.66 (d, 1H, J=6.9 Hz, Ar–H). ^{13}C NMR ($CDCl_3$) δ: 21.5 (q), 23.7 (br), 46.8 (br), 51.5 (br), 116.6 (d), 127.9 (d), 128.6 (d), 130.9 (d), 136.7 (s), 137.9 (d), 138.1 (d), 152.2 (s), 153.0 (s), and 154.3 (s). Electron ionization-mass spectrometry (EI-MS) *m/z*: 474 (M^+-*p*Tol), *anal.* (%) calcd. for $C_{24}H_{26}BiN_3$: C, 50.98; H, 4.63; N, 7.43; found: C, 50.93;H, 4.58; N, 7.40.

2.2. X-ray crystal structural determinations of **3** and **4**

X-ray data was collected on a Bruker APEX II diffractometer with a CCD detector with graphite monochromated radiation (MoKα, λ = 0.71073 Å) at 120 K. Empirical absorption correction was applied to the collected reflections with SADABS and the space group was determined using XPREP. The structure was solved by the direct methods using SHELXS-97 and refined on F2 by full-matrix least-squares using the SHELXL-97 program package [22]. All hydrogen atoms were included in calculated positions and treated as riding atoms by using default SHELXL parameters (Table 1).

2.3. Reagents

The organometallic compounds (**1**–**4**) used in this study are shown in Fig. 1. They were resolved in DMSO at 50 mM and stocked at −80 °C prior to use. Hydroxyphenyl fluorescein (HPF) was purchased from Sekisui Medical (Tokyo, Japan); the WST-8 assay kit from Kishida (Osaka, Japan); and Annexin V-HiLyte Fluor™ 488 from AnaSpec International (San Jose, CA, USA). All other reagents were from Sigma or Wako Chemicals (Osaka, Japan) and of the highest quality commercially available.

2.4. Cells and culture

All the human cancer cell lines, except NB4 and TIG cell lines, used in this study were obtained from the American Type culture Collection (Manassas, VA, U.S.A.). TIG-3 was obtained from Japanese Collection of Research Bioresource (Osaka, Japan) and NB4 was kindly provided by Dr. Junko Kado (Saitama Cancer Center Research Institute, Saitama, Japan). K562, NB4 and HL60 cells were cultured in standard culture conditions (37 °C, 95% air: 5% CO_2) in RPMI1640 medium (Nissui; Tokyo, Japan) supplemented with 10% fetal bovine serum (Gibco),

Table 1
Crystal data and structure refinement parameters for compounds **3** and **4**.

Parameters	**3** (M = Sb)	**4** (M = Bi)
Empirical formula	$C_{24}H_{26}N_3Sb$	$C_{24}H_{26}N_3Bi$
Formula weight	478.23	565.46
Temperature (K)	120	120
Crystal size (mm)	0.18×0.13×0.10	0.21×0.10×0.10
Crystal system	Orthorhombic	Monoclinic
Space group	Pbca	P21/c
a (Å)	17.5856(12)	17.255(2)
b (Å)	9.1101(6)	5.8701(7)
c (Å)	27.2491(18)	21.926(3)
α (°)	90	90
β (°)	90	102.908(2)
γ (°)	90	90
V (A^3)	4365.5(5)	2164.7(4)
Z	8	4
Density (Mg/m^3)	1.455	1.735
F(000)	1936	1096
Reflections collected	20,448	12,537
Independent reflections	4540	4935
R(int)	0.0231	0.0444
Goodness-of-fit on F^2	1.017	1.036
R1, wR2 [I>2σ(I)]	0.0224, 0.0512	0.0317, 0.0648

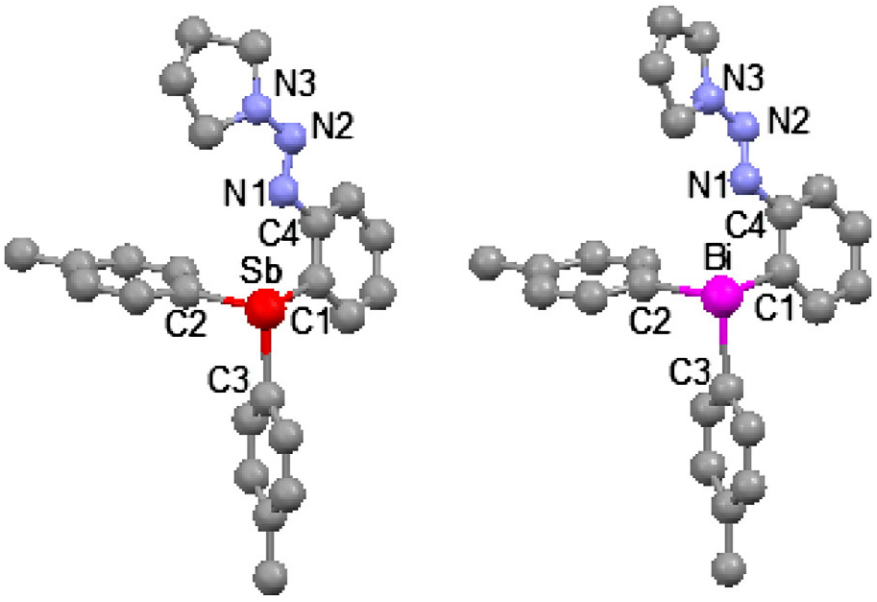

Fig. 1. Molecular structure of **3** (Sb) and **4** (Bi). (Hydrogens are omitted.)

2 mM L-glutamine and 1% penicillin–streptomycin. Other human cancer cell lines were cultured in DMEM (Nissui) supplemented with 10% fetal bovine serum (Gibco), 2 mM L-glutamine and 1% penicillin–streptomycin at 37 °C under 5% CO_2.

2.5. Quantitation of metals accumulated in cells

Cells were cultured in 100-mm dishes and treated with the organobismuth compound or organoantimony compound for 3 h. The monolayer was washed two times with phosphate-buffered saline (PBS) (0.5 ml of SDS buffer (50 mM Tris, 2% SDS, 10% glycerol, pH 6.8) was added to each dish, and the cells were lysed and collected into microtubes. The tubes were incubated for 10 min at 95 °C. The lysate of 100 μl was digested at 130 °C for 2 days with nitric acid–H_2O_2 in an aluminum dry-block bath. The samples were diluted with 0.1 N nitric acid and the antimony or bismuth concentration was measured by inductively coupled plasma mass spectrometry (inductively coupled plasma mass spectrometry (ICP-MS), ELAN DRC II, PerkinElmer, MA USA).

2.6. Analysis of inhibition of cell growth

The cytotoxity of organometallic compounds in human cancer cell lines was determined by the WST-8 assay [23] using a modified method according to the manufacturer's instructions. In all assays, the compounds were dissolved in DMSO and diluted in sterile culture medium immediately before addition to the cell culture, and the concentration of DMSO did not exceed 0.1% (v/v). The cells (1×10^5/ ml) were seeded in 96-well plates. After 12 h, various concentrations of **1**–**3** or **4** (0.001 μM–10 μM in case for **1**–**3**; 0.001 μM–20 μM for **4**) were added. After 12 h treatment, WST-8 was added and the plates were incubated for an additional 4 h. The medium was discarded and the formazane blue that formed in the cells was dissolved with 100 μl of DMSO. The optical density was measured at 570 nm.

2.7. Apoptosis quantified by FACS analysis

Apoptosis was assessed by annexin-V staining and propidium iodide exclusion using methods described previously [23]. After treatment with the indicated concentrations of compounds for 12 h, cells were harvested and cell pellets were resuspended in a staining solution containing annexin V-HiLyte Fluor 488 and then stained with propidium iodide. Cells were analyzed with a Becton-Dickinson FACSCalibur flow cytometer.

2.8. Determination of intracellular ROS production

ROS were detected using hydroxyphenyl fluorescein (HPF). HPF fluoresces upon reacting with highly reactive oxygen species (hROS) [25]. Briefly, NB4 cells (1×10^5/ml)were pretreated with 10 μM HPF for 30 min. Then the compound was added and the culture was continued for 1 h at 37 °C. After incubation, the cells were pelleted by centrifugation at 2500 rpm for 3 min, resuspended in 500 μl of phosphate-buffered saline (PBS) and analyzed with the flow cytometer.

2.9. Assay of microtubule assembly in vitro

The assembly of porcine tubulin was monitored using porcine brain tubulin purified as described earlier [24]. Tubulin was resuspended on ice in ice-cold tubulin-polymerization buffer (80 mM piperazine-1, 4-bis (2-ethane sulfonic acid (PIPES) pH 6.9, 2 mM $MgSO_4$, 1 mM ethylene glycol tetra acetic acid (EGTA), 1 mM Mg-GTP, and 1.5% (v/v) glycerol) and 100 μl (250 μg) was pipetted into the designated wells of a half area 96-well plate pre-warmed to 25 °C in 0.20 mM of each compound. The assay was conducted at 25 °C, and tubulin polymerization was monitored at 340 nm in a Multiscan micro plate reader (Thermo Labsystems, Franklin, MA, USA). The increase in absorbance was measured at 340 nm at 25 °C and recorded every 30 s for 30 min.

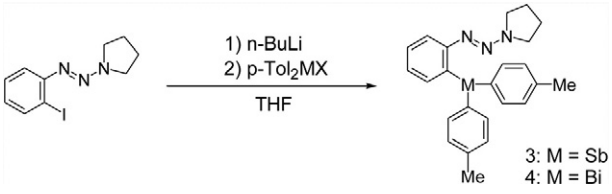

Scheme 1. Synthesis of the organoanitimony **3** and organobismuth **4**.

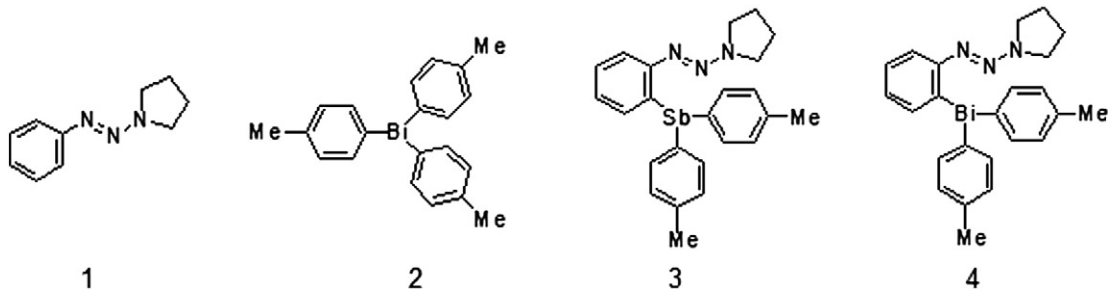

Fig. 2. Chemical structure of the compounds.

2.10. Assessment of mitochondrial membrane potential ($\Delta\Psi_{mt}$)

NB4 cells (1×10^5/ml) were incubated in the absence or presence of the organobismuth compounds. The cells were harvested at 6 h post-treatment, pelleted by centrifugation at 2500 rpm for 3 min, resuspended in 500 μl of rhodamine 123 (20 μg/ml) and incubated for 15 min at 37 °C. After washing with PBS, cells were resuspended in PBS and analyzed with the flow cytometer.

2.11. Statistical analysis

All the results were expressed as the mean ± S.D. for data obtained from at least three separate experiments. Data were analyzed for statistical significance by the paired *t* test, and $P<0.05$ was considered to indicate statistically significant differences.

3. Results

3.1. Synthesis and molecular structure of organoantimony and organobisumuth compounds 3, 4

The synthesis of novel organoantimony and organobisumuth compounds having a triazene moiety, 1-[2-(di-p-tolylstibanophenyl) diazenyl]pyrrolidine (**3**) and 1-[2-(di-p-tolylbismuthanophenyl) diazenyl]pyrrolidine (**4**), is shown in Scheme 1. 1-[(2-iodophenyl) diazenyl]pyrrolidine [26] was treated with n-BuLi in anhydrous THF at −78 °C under an argon atomosphere, followed by trapping with an electrophilic metal reagent [p-Tol_2SbBr and p-Tol_2BiCl] to give **3** and **4**, respectively, in 40 and 48% yields.

The molecular structures of **3** and **4** are confirmed by their elemental analyses and spectral techniques (^{1}H and ^{13}C NMR, MS). Crystal structures of **3** and **4** are shown in Fig. 2, and selected bond lengths and angles are listed in Table 2. The N═N double bonds in diazoamino group (–N═N–N<) of **3** and **4** adopt a trans configuration, and the N1═N2 bond distances [3 (M═Sb): 1.278(2) Å, 4 (M═Bi): 1.260(7) Å] are larger than the typical value for N═N bond (1.25 Å). On the other hand, N2–N3 bonds [3 (M═Sb): 1.315(2) Å, 4 (M═Bi): 1.318(7) Å] and N1–C4 bonds [3 (M═Sb): 1.420(3) Å, 4 (M═Bi): 1.426(7) Å] are shorter than the typical single N–N (1.45 Å) and N–C bonds (1.47 Å) [27], respectively. These deviation of N═N, N–N and N–C bond lengths indicate a delocalization of the π and n electrons on triazene group. Intramolecular interaction between pnictogen elements (in particular Sb, Bi) and nitrogen atoms has attracted interest [28]. We also have reported that triarylstibane and bismuthane derivatives frequently interact with nearly nitrogen, producing Sb, Bi···N intramolecular coordination [29–31]. In the case of **3** and **4** having triazene moiety, intramolecular interaction was absent between antimony/bismuth and nitrogen (N2) in solid-state: the spatial distances of Sb–N2 and Bi–N2 are 4.235(2) Å (3: Sb) and 4.257(5) Å (4: Bi) which corresponds to 113% and 108% of the sum of the van der Waals radii of both elements (N–Sb: 3.74 Å, N–Bi: 3.94 Å) [27]. The central antimony and bismuth atoms exhibit a pyramidal structure, and the three M–C bond lengths and the bond angles (C–M–C) surrounding of antimony and bismuth were similar to trivalent organoantimony and bismuth such as triphenylstibane (2.143–2.169 Å, 95.1–98.0°) [32] and triphenylbismuthane (2.237–2.273 Å, 92.7–94.7°) [33].

Table 2
Selected bond distances (Å) and angles (°) for triazene compounds **3** and **4**.

3 (M═Sb)		**4** (M═Bi)	
N1–N2	1.278(2)	N1–N2	1.260(7)
N2–N3	1.315(2)	N2–N3	1.318(7)
N1–C4	1.420(3)	N1–C4	1.426(7)
Sb–C1	2.151(2)	Bi–C1	2.240(6)
Sb–C2	2.150(2)	Bi–C2	2.263(5)
Sb–C3	2.163(2)	Bi–C3	2.274(6)
Sb–N1	2.989(2)	Bi–N1	3.027(5)
Sb–N2	4.235(2)	Bi–N2	4.257(5)
Sb–N3	4.757(2)	Bi–N3	4.736(5)
C1–Sb–C2	95.38(7)	C1–Bi–C2	95.1(2)
C1–Sb–C3	96.28(7)	C1–Bi–C3	92.3(2)
C2–Sb–C3	95.96(7)	C2–Bi–C3	91.98(19)

3.2. Cytotoxic activity

Cytotoxic effects of the compounds depicted in Fig. 2 on NB4 cells were examined using the WST-8 assay. As shown in Fig. 3, **4** in which a phenylmethyl was changed to a phenyldiazenyl exhibited strong antiproliferative activity; the viability of NB4 cells was decreased at a concentration of more than 0.1 μM. On the other hand, compounds **1**–**3** exerted only a weak anti-proliferative effect up to a concentration of 10 μM. The cytotoxic effect of **1–3** could not be determined above 10 μM, because limited solubility resulted in the precipitation of the compound which had an apparent effect on cell viability. Compound **2**, tri(*p*-tolyl)bismuthane, showed only a weak cytotoxic

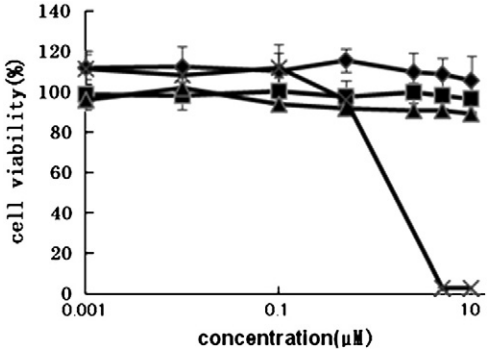

Fig. 3. Cell viability assay. Viability of NB4 cells after exposure for 12 h at 37 °C to increasing concentrations of **1** (▲), **2** (■), **3** (♦), or **4** (×). Viability was determined by WST-8 assay. Each point is the mean ± S.D. for three different experiments performed in triplicate.

activity toward NB4 cells. This result is consistent with previous toxicological results for this compound including low cytotoxicity in vascular endothelial cells [19,34]. Arata et al. also reported that 30 μM of triphenylbismuth was needed to achieve clear cytotoxic effect on rat thymocytes [35]. Unexpectedly, **3**, the compound containing antimony in place of bismuth, showed no cytotoxic activity up until 10 μM either.

Next, 50% growth inhibition (IC_{50}) values of **4** for various human cancer cell lines and normal fibroblast cells (TIG) were determined at concentrations of 0.001 μM–20 μM (Table 3). Leukemia cell lines were relatively sensitive compared to other cell lines. Among the leukemia cell lines tested, NB4 cells were the most sensitive. The IC_{50} of **4** (0.88 μM) for NB4 cells was low compared to that of the heterocyclic organobismuth(III) (bi-chlorodibenzo[*c,f*][*1,5*]thiabismocine) compound that exhibited potent bioactivity against human cancer cell lines (IC_{50} = 0.05–0.25 μM) [18].

We next examined the time course of cytotoxic effect of **4** on NB4, K562, and HeLa cells, respectively, at each IC_{50} concentration (Fig. 4). The viability of control culture increased during the culture because of cell proliferation. On the other hand, the treatment with **4** inhibited the proliferation of all the cell lines examined, and further reduced their viability time-dependently.

3.3. Accumulation of the compounds in NB4 cells

As shown in Fig. 3, the toxicity study indicated the antimony compound **3** to show no activity, although **4** was active. To explain this difference in cytotoxic activity, the accumulation of metals in treated cells was examined. After treatment with **4** or **3** at 0.88 μM for 1 h, the amount of bismuth or antimony accumulated in NB4 cells was determined using luminescence FT-IR. The amount of bismuth was 53.22 ± 2.74 fmol/μg DNA, but that of antimony in the **3**-treated cells was only 0.75 ± 0.49 fmol/μg DNA. Tests were performed using other organometallic compounds and the results indicated that the bismuth compounds were more cytotoxic and caused more accumulation in cells than the corresponding antimony compounds. The reason for this difference is unknown.

3.4. Apoptosis induction

To verify whether cell damage is attributable to the induction of apoptosis, NB4 cells were treated for 12 h with the indicated concentrations of compound and then the ratio of apoptotic cells was determined by estimating FITC-labeled annexin-V binding to phosphatidylserine, as diagnostic of apoptosis [36] (Fig. 5). As shown in Fig. 5A and B, the ratio of apoptotic NB4 cells treated with **1** or **2** did not increase compared with the non-drug control culture. On the other hand, **4** began to induce apoptosis at around its IC_{50} and there was a concentration-dependent increase in the population of cells in apoptosis (Fig. 5C). We also examined the induction of apoptosis by counting cells that exhibited typical apoptotic morphological changes (i.e., condensed nuclei and chromatin fragmentation) under the fluorescence microscope and obtained the similar results with those as the annexin-V labeling procedure.

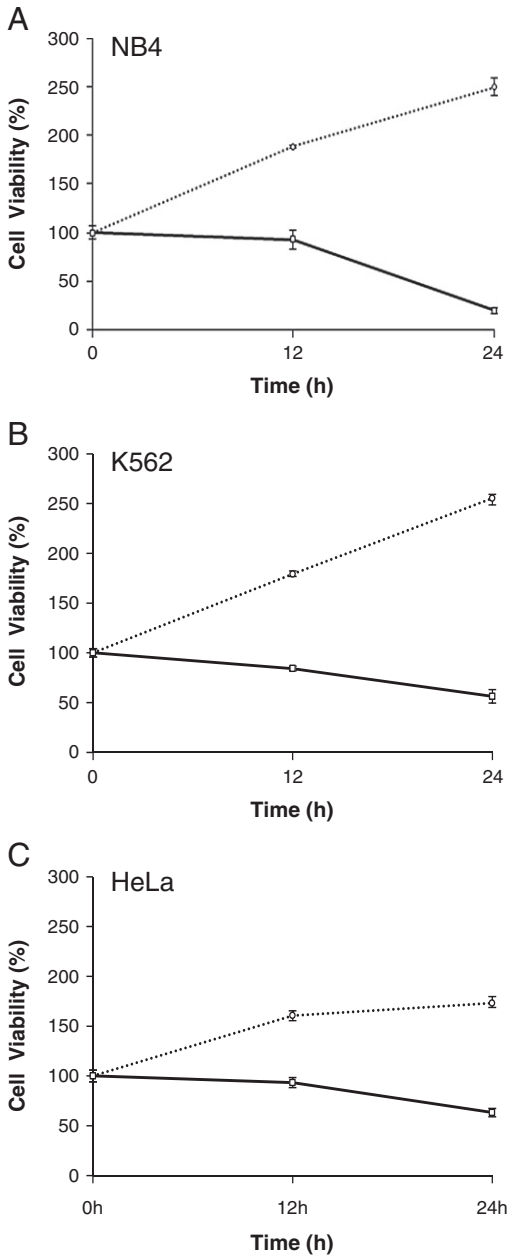

Fig. 4. Time course of cytotoxic effect of **4**. NB4 (A), K562 (B) and HeLa (C) cells were treated for the indicated times with each IC_{50} value of **4** (NB4, 0.88 μM; K562, 3.33 μM; HeLa, 5.36 μM). Cell viability was examined using WST-8 assay. Cell treatments were as follows: ○ (dashed line), control; □, treated with IC_{50} value for each cell line. Each point is the mean ± S.D. for three different experiments performed in triplicate.

Table 3
Cytotoxic activity of triazene compound **4** in several human cancer cell lines.

Human tumor type	Cell line	IC_{50} (μM)[a]
Leukemia	NB4	0.880 ± 0.102[b]
	K562	3.331 ± 0.932
	HL60	1.445 ± 0.034
Breast cancer	MDA-MB-435S	3.344 ± 0.574
Colon cancer	DLD-1	3.501 ± 1.106
Pancreatic cancer	MIA paca	2.589 ± 0.011
Lung cancer	A549	3.344 ± 0.574
Osteosarcoma	MG-63	4.830 ± 0.510
Fibrosarcoma	HT1080	8.478 ± 0.297
Cervical cancer	HeLa	5.360 ± 0.534
Normal human cell fibroblasts	TIG-3	7.716 ± 1.323

[a] IC_{50} was obtained through the 4 Parameter Logistic nonlinear regression model.
[b] ±, standard deviation of three independent experiments.

3.5. Compound 4 increases in ROS levels and reduces mitochondrial membrane potential disruption($\Delta\Psi_{mt}$)

In an attempt to gain insight into the molecular basis of the cytotoxic effect of **4**, we first examined whether ROS levels were increased. ROS has been shown to play important roles in the initiation and

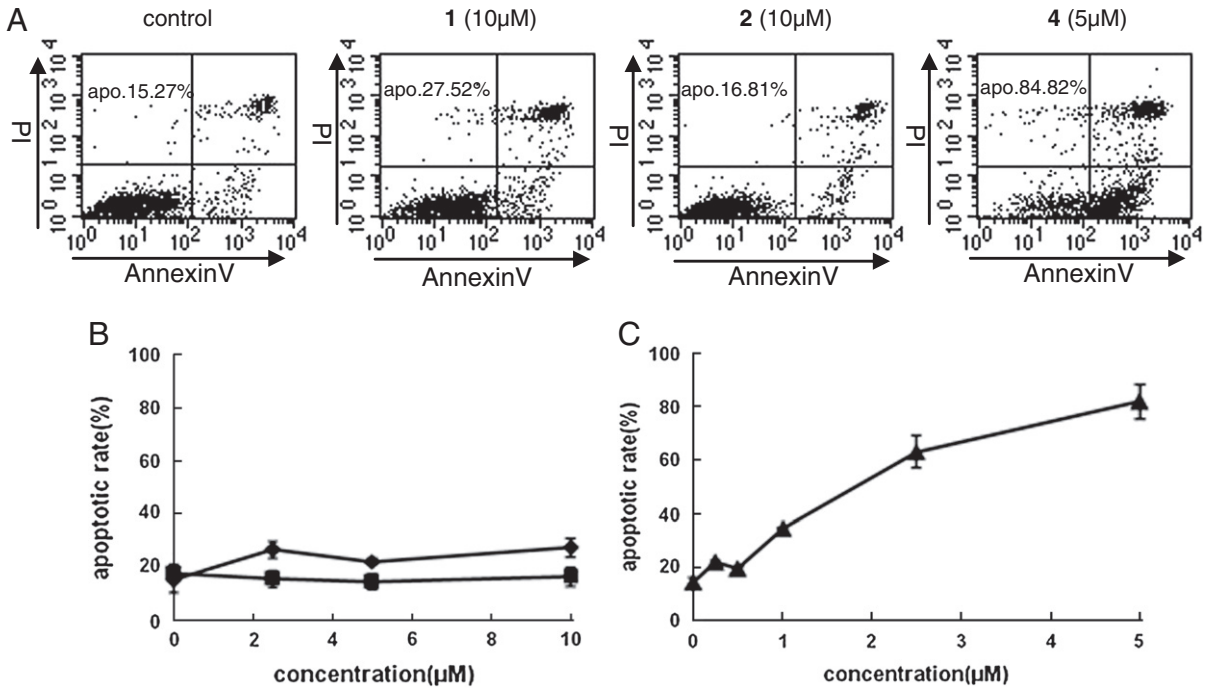

Fig. 5. Induction of apoptosis. Representative annexin-V/PI bivariate dot-blot figures displaying apoptotic NB4 cells after treatment with **1**, **2** or **4** for 12 h at the concentration depicted under the figure (A). Apoptotic cells were detected by the annexin-V and propidium iodide (PI) method. Annexin-V and PI stainings were measured by flow cytometry. *X* axis, the fluorescent intensity of Annexin-V. *Y* axis, the fluorescent intensity of PI. The upper right quadrant shows later apoptotic and necrotic cells and the lower right quadrant, early apoptotic cells. Total percentages of the Annexin-V-positive, PI-negative cells plus both positive cells, are shown in each panel as a percentage of apoptotic cells. Percentage of apoptotic cells after 12 h treatment with increased concentrations of **1** (⬥) or **2** (■) (B), or 4 (▲) (C). Rate of apoptotic cells quantified by flow cytometry as shown in (A). Each point is the mean ± S.D. for three different experiments performed in triplicate.

execution of apoptosis [18,37]. ROS production was evaluated with a fluorescent probe, 2-[6-(4′-hydroxy)phenoxy-3*H*-xanthen-3-on-9-yl]benzoic acid (HPF). HPF detects highly reactive oxygen species (hROS) such as the hydroxyl radical (OH) and reactive intermediates of peroxidase and is resistant to light-induced autoxidation, unlike DCFH-DA [38]. As shown in Fig. 6, the treatment of NB4 cells with **4** increased ROS levels ($P<0.05$ vs. control). However the ROS level was not significantly changed by the 12 h treatment with **1** or **2**. Our previous study has shown that caspase activation, a key process in apoptosis, followed a loss of $\Delta\Psi_{mt}$ [18]. Thus, we next examined changes in $\Delta\Psi_{mt}$ after the 12 h treatment with bismuth compounds. As summarized in Fig. 7, **4** caused a marked loss of $\Delta\Psi_{mt}$ as compared with **1** or **2** in treated cells. Taken together, these results support the idea that **4** induces apoptosis in NB4 cells by a ROS-mediated pathway, as we have previously demonstrated in the case of a heterocyclic organobismuth (III) compound [18].

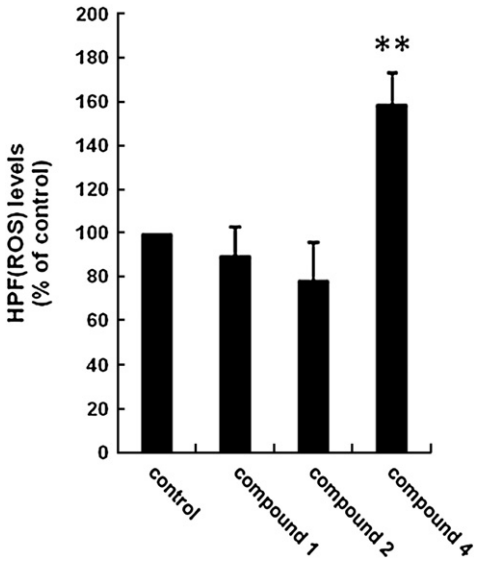

Fig. 6. ROS production in NB4 cells treated with organobismuth compounds. An increase in intracellular peroxide production in NB4 cells treated with **1**, **2**, or **4** was determined by flow cytometric analysis using DCHF-DA as a fluorescent dye. Cells were treated with a concentration of two-fold the IC_{50} of each compound for 12 h. The ROS generated are indicated as a relative value against the control ROS production. Data are expressed as % and are the mean ± S.D. for three different experiments performed in triplicate. $^{**}P<0.01$ versus control.

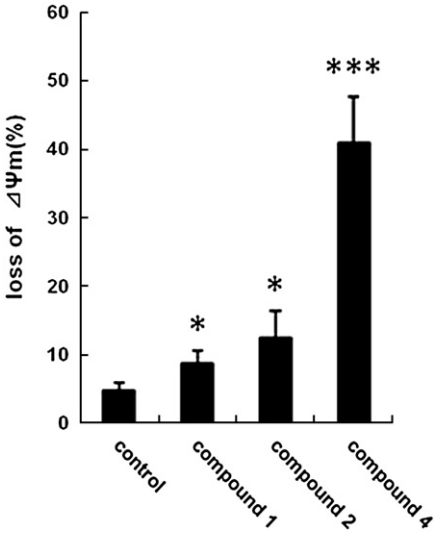

Fig. 7. Mitochondrial membrane potential disruption. Cells were cultured with different organobismuth compounds at a concentration of two-fold the IC_{50} value for 12 h, then stained with rhodamine 123 and analyzed immediately by flow cytometry. The number indicates the percentage of cells with reduced $\Delta\Psi_{mt}$. Data are expressed as % and are the mean ± S.D. for three different experiments performed in triplicate. $^{*}P<0.05$, $^{***}P<0.001$ versus control.

3.6. Suppression of **4**-induced ROS production and apoptosis by cotreatment with antioxidant, N-acetyl-cysteine (NAC)

Next, we designed experiments to determine whether **4**-induced ROS generation and apoptotic cell death were attenuated by NAC, an antioxidant [39]. The present results showed that pretreatment with NAC conferred significant protection against 4-induced ROS production and apoptosis in NB4 cells (Fig. 8).

3.7. Inhibition of tubulin polymerization in vitro

We have previously shown that heterocyclic organobismuth(III) targets tubulin resulting in depolymerization *in vitro* and destroys the microtubular network of HeLa cells [24]. Microtubules function in a number of cellular processes and numerous anti-tumor drugs have been known to target microtubules [40]. Many heavy metal compounds have also been shown to damage microtubules [41]. Then, we examined the effect of three compounds on the assembly of tubulin subunits into microtubules *in vitro*. As shown in Fig. 9, **1** and **4** did not affect tubulin polymerization, whereas nocodazole, a positive control drug, inhibited it. In accordance with these results, neither of these two compounds disrupted the cellular microtubule network of HeLa cells treated with their IC_{50} concentrations for 12 h (data not shown).

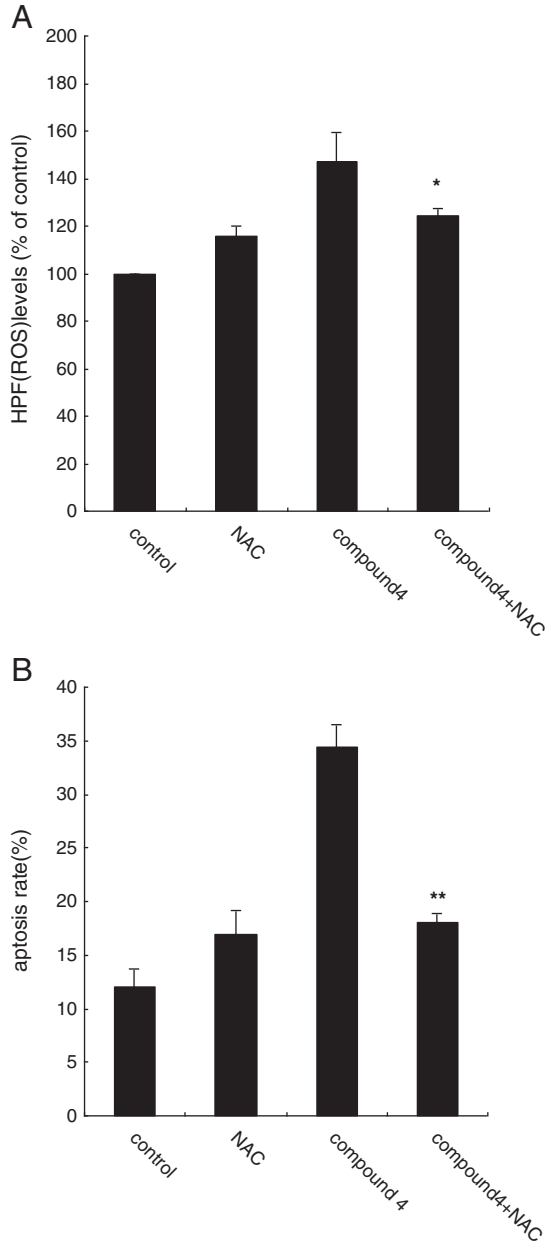

Fig. 8. NAC protected against 4-induced ROS production and apoptosis. NB4 cells were cultured in the absence or presence of 10 mM NAC for 2 h, and then, exposed to 1.8 μM ($2\times IC_{50}$) **4** alone or in combination of NAC for 12 h. ROS production was determined by flow cytometric analysis using DCHF-DA (A). Apoptotic cells were detected by the annexin-V and propidium iodide (PI) method (B). In panels, results are mean ± S.D. for three different experiments performed in triplicate. $^{*}P<0.05$, $^{**}P<0.01$ versus compound **4**.

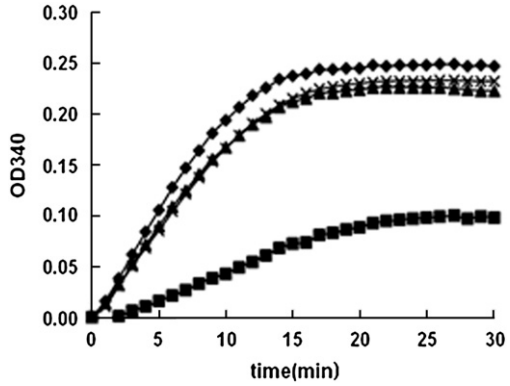

Fig. 9. Inhibition of tubulin polymerization *in vitro*. Organobismuth compounds inhibited tubulin assembly *in vitro*. MAP-rich tubulin in a reaction buffer was incubated at 25 °C in the presence of DMSO (control, 0.01% ◆), nocodazole (20 μM) (■), **1** (▲) and **4** (×) (25 μM, each). The polymerization of tubulin was determined by measuring the increase in absorbance over time at 340 nm.

4. Discussion

We describe the synthesis of a novel organobismuth (III) with the diazenyl pyrrolidine **4** and revealed that the tri(*p*-tolyl) bismuthane **2** can be modified from an inactive to highly toxic compound against human cancer cell lines by the introduction of a diazenyl pyrrolidine at the *ortho* position of one of the benzene rings. Bismuth compounds, especially pentavalent organobismuth compounds, have been known to serve as an oxidant under mild conditions in organic chemistry [42]. However, the mechanism of action of the organobismuth compound in cells is not fully resolved. Inorganic bismuth(III) compounds, like bismuth subsalicylate, were reported to make a complex with cysteine or glutathione (GSH) *in vitro* [43,44]. As has been shown, GSH is used as a reducing substrate for the function of glutathione peroxidase in cells [45]; it can be supposed that the change in cellular GSH content affected the intracellular redox environment and resulted in the elevation of ROS levels [18]. However, our preliminary experiments with heterocyclic organobismuth(III) using an *in vitro* assay system with GSH as substrate did not show any evidence of the direct inhibition of glutathione peroxidase activity. In addition, we have revealed that one specific biological target of heterocyclic organobismuth(III) is tubulin [24]. However, as shown in Fig. 9, **4** is not a tubulin-disrupter. Thus, an unknown target of **4** should exist to trigger apoptosis. In this respect, the diazenylpyrrolidine moiety would be important to the bioactivity of **4** because compounds with the triazene structure are known to have antimalarial activity [16]. Several drugs for cancer undergo metabolic conversion and their metabolites are significantly more toxic to cancer cells [46,47]. Triazene compounds also are known to activate through a metabolic pathway [14,48]. Although **4** shows high a degree of stability during synthesis and purification, some metabolic activation cannot be excluded.

5. Conclusion

In conclusion, introduction of the triazene structure (–N═N – NR_2) into a benzene ring of tri(*p*-tolyl)bismuthane gave potent cytotoxic activity against human tumor cell lines through the induction of apoptosis. The results of this study should aid the development of organometallics-based drugs for leukemia because compounds with multiple intracellular targets designed using the pharmacophore model would be more effective against drug-resistant tumors.

Acknowledgments

Partial financial support for this work was provided by a grant-in aid for Scientific Research (J. K.) from the Ministry Education, Sciences, Sports and Culture of Japan, and Special Research Found from Hokuriku University.

Appendix A. Supplementary data

Supplementary data are available from the CCDC, 12 Union Road, Cambridge CB2 1EZ, U.K., e-mail: deposit@ccdc.cam.ac.uk, on request, quoting the deposition nos. CCDC 882185 (3) and 882186 (4) respectively.

References

[1] Y.F. Shealy, C.A. Krauth, Nature 210 (1966) 208–209.
[2] S.K. Carter, M.A. Friedman, Eur. J. Cancer 8 (1972) 85–92.
[3] R.C.S. Audette, T.A. Connors, H.G. Mandel, K. Merai, W.C.J. Ross, Biochem. Pharmacol. 22 (1973) 1855–1864.
[4] F.A. Schmid, D.J. Hutchison, Cancer Res. 34 (1974) 1671–1675.
[5] S.M. Lee, N. Thatcher, D. Crowther, G.P. Margison, Br. J. Cancer 69 (1994) 452–456.
[6] B.J. Jean-Claude, A. Mustafa, N.D. Cetateanu, Z. Damian, J. De Marte, R. Yen, D. Vasilescu, T.H. Chan, B. Leyland-Jones, Br. J. Cancer 76 (1997) 467–473.
[7] S.L. Matheson, J. Mcnamee, B.J. Jean-Claude, J. Pharmacol. Exp. Ther. 296 (2001) 832–840.
[8] T. Cimbora-Zovko, A. Brozovic, I. Piantanida, G. Fritz, A. Virag, B. Alic, V. Majce, M. Kocevar, S. Polanc, M. Osmak, Eur. J. Med. Chem. 46 (2011) 2971–2983.
[9] A. Franchi, G. Papa, S. D'Atri, D. Piccioni, M. Masi, E. Bonmassar, Haematologica 77 (1992) 146–150.
[10] K. Seiter, D. Liu, T. Loughran, A. Siddiqui, P. Baskind, T. Ahmed, J. Clin. Oncol. 20 (2002) 3249–3253.
[11] M. Turriziani, P. Caporaso, L. Bonmassar, F. Buccisano, S. Amadori, A. Venditti, M. Cantonetti, S. D'Atri, E. Bonmassar, Pharmacol. Res. 53 (2006) 317–323.
[12] R. Preussman, H. Druckrey, S. Ivankovic, A. von Hodenberg, Ann. N. Y. Acad. Sci. 163 (1969) 697–716.
[13] J.L. Skibba, D.D. Beal, G. Ramirez, G.T. Bryan, Cancer Res. 30 (1970) 147–150.
[14] J.M. Reid, M.J. Kuffel, J.K. Miller, R. Rios, M.M. Ames, Clin. Cancer Res. 5 (1999) 2192–2197.
[15] M. Bower, E.S. Newlands, N.M. Bleehen, M. Brada, R.J. Begent, Cancer Chemother. Pharmacol. 40 (1997) 484–488.
[16] K. Nishiwaki, A. Okamoto, K. Matsuo, Y. Kawaguchi, Y. Hayase, K. Ohba, Bioorg. Med. Chem. 15 (2007) 2856–2859.
[17] T. Kotani, D. Nagai, K. Asahi, H. Suzuki, F. Yamao, N. Kataoka, T. Yagura, Antimicrob. Agents Chemother. 49 (2005) 2729–2734.
[18] K. Iuchi, Y. Hatano, T. Yagura, Biochem. Pharmacol. 76 (2008) 974–986.
[19] T. Yagura, Res. Adv. Antimicrob. Chemother. 6 (2006) 19–32.
[20] N.I. Foster, Synthesis (1980) 572–573.
[21] S. Combes, J.-F. Finet, Synth. Commun. 26 (1996) 4569–4575.
[22] G.M. Sheldrick, Acta Crystallogr. A64 (2008) 112–122.
[23] M. Ishiyama, Y. Miyazono, K. Sasamoto, Y. Ohkura, K. Ueno, Talanta 44 (1997) 1299–1305.
[24] K. Iuchi, K. Akagi, T. Yagura, J. Pharmacol. Sci. 109 (2009) 573–582.
[25] K. Setsukinai, Y. Urano, K. Kakinuma, H.J. Majima, T. Nagano, J. Biol. Chem. 278 (2003) 3170–3175.
[26] M.L. Bell, R.C. Chiechi, C.A. Johnson, D.B. Kimball, A.J. Matzger, W.B. Wan, T.J.R. Weakley, M.M. Haley, Tetrahedron 57 (2001) 3507–3520.
[27] J. Emsley, The Elements, Third ed. Clarendon Press, Oxford, 1998.
[28] K.-y. Akiba, Chemistry of Hypervalent Compounds, VCH, New York, 1999.
[29] T. Tokunaga, H. Seki, S. Yasuike, M. Ikoma, J. Kurita, K. Yamaguchi, Tetrahedron 56 (2000) 8833–8839.
[30] S. Yasuike, Y. Kishi, S. Kawara, K. Yamaguchi, J. Kurita, J. Organomet. Chem. 691 (2006) 2213–2220.
[31] M. Kawahata, S. Yasuike, I. Kinebuchi, K. Yamaguchi, J. Kurita, Acta Crystallogr. E67 (2011) m25.
[32] E.A. Adams, J.W. Kolis, W.T. Pennington, Acta Crystallogr. C46 (1990) 917–919.
[33] P.G. Jones, A. Blaschette, D. Henschel, A. Weitze, Z. Kristallogr. 210 (1995) 377–378.
[34] Y. Fujiwara, M. Mitani, S. Yasuike, J. Kurita, T. Kaji, J. Health Sci. 51 (2005) 333–340.
[35] T. Arata, Y. Oyama, K. Tabaru, M. Satoh, H. Hayashi, S. Ishida, Y. Okano, Environ. Toxicol. 17 (2002) 472–477.
[36] M. Vanengeland, L.J.W. Nieland, F.C.S. Ramaekers, B. Schutte, C.P.M. Reutelingsperger, Cytometry 31 (1998) 1–9.
[37] C. Fleury, B. Mignotte, J.L. Vayssiere, Biochimie 84 (2002) 131–141.
[38] J.A. Royall, H. Ischiropoulos, Arch. Biochem. Biophys. 302 (1993) 348–355.
[39] I.A. Cotgreave, Adv. Pharmacol. 38 (1997) 205–227.
[40] M.A. Jordan, L. Wilson, Nat. Rev. Cancer 4 (2004) 253–265.
[41] I.N. Chou, Biomed. Environ. Sci. 2 (1989) 358–365.
[42] In: H. Suzuki, Y. Matano (Eds.), Organobismuth Chemistry, Elsevier, Amsterdam, The Netherlands, 2001.
[43] N. Burford, M.D. Eelman, D.E. Mahony, M. Morash, Chem. Commun. 7 (2003) 146–147.
[44] P.J. Sadler, H. Sun, H. Li, Chem. Eur. J. 2 (1996) 701–708.
[45] I.A. Cotgreave, P. Moldeus, R. Brattsand, A. Hallberg, C.M. Andersson, L. Engman, Biochem. Pharmacol. 43 (1992) 793–802.
[46] H.V. Aposhian, Annu. Rev. Pharmacol. Toxicol. 37 (1997) 397–419.
[47] C. Rodriguez-Antona, M. Ingelma-Sundberg, Oncogene 25 (2006) 1679–1691.
[48] B.L. Pool, J. Cancer Res. Clin. Oncol. 93 (1979) 221–231.